4950 *Macromolecules* **2009**, *42*, 4950–4952
DOI: 10.1021/ma901014m

Macromolecules
COMMUNICATION TO THE EDITOR

Morphology Transition in RAFT Polymerization for Formation of Vesicular Morphologies in One Pot

Wen-Ming Wan, Xiao-Li Sun, and Cai-Yuan Pan*

Department of Polymer Science and Engineering, CAS Key Laboratory of Soft Matter Chemistry, University of Science and Technology of China, Hefei, Anhui 230026, P. R. China

Received May 9, 2009
Revised Manuscript Received June 23, 2009

Vesicular nanostructural materials have displayed potential applications in various fields such as in catalysis, biomedical, cosmetic, and food industries.[1] So their preparation attracted much attention in the past decade, and the conventional strategy for preparation of the vesicles is self-assembling of amphiphilic block copolymers in a selective solvent, which is performed by slowly adding a precipitant of hydrophobic chains into a polymer solution for inducing their aggregation.[2] Essentially the variable in this process is the solvent parameter (δ) because the polymers used have fixed molecular weight and fixed chain length ratio of hydrophobic to hydrophilic blocks. But this strategy is difficult to control, is time-consuming, and involves multiple steps.[3] Thus, great efforts have been paid to study the direct chemical preparation of various polymeric nanostructures. One approach is controlled radical polymerization in a selective solvent, which is so-called polymerization-induced self-assembling, but only spherical micelles were always produced.[3−5] So, the question is: could these vesicular morphologies, which are formed by self-assembly of the block copolymers in a selective solvent, be prepared via polymerization? In this Communication, we report a facile and feasible approach to prepare vesicular nanomaterials via controlled radical polymerization.

In studying the effect of chain length ratio of polystyrene (PS) to poly(acrylic acid) (PAA) on morphologies including spherical micelles, rodlike micelles, and vesicles formed by self-assembling of PS-*b*-PAA, the polymers with the lowest chain length ratio of PS to PAA produced spherical micelles.[6] In the polymerization-induced self-assembling, the hydrophobic chains grow to a critical chain length for phase separation, which always met requirement for formation of spherical micelles. So it is understandable that the controlled radical polymerization in a selective solvent formed always spherical micelles. Thus, a key point for preparation of vesicular morphologies is how to transform the spherical micelles into the desired morphologies.

Theoretically, morphology is mainly controlled by a force balance involving stretching of the core chains, surface tension between the core and the outside solvent, and repulsion among the corona polymer chains.[7] So, altering the force balance may induce the morphology transition, which can be achieved by greatly increasing the core chain length or appropriate selection of solvent. Our previous results showed that the propagation rate of core chains in the micelles was very slow, but a fast rate was observed in a comparatively good solvent of the core block.[4] This may be due to high mobility of the core chains, and fast diffusion rate of the monomer from outside into the micelles may be another reason. Thus, we designed a polymerization system where the reversible addition−fragmentation transfer (RAFT) polymerization of styrene (St) was performed in methanol using *S*-1-dodecyl-*S*-(α,α'-dimethyl-α''-acetic acid)trithiocarbonate (TC)-terminated poly(4-vinylpyridine) (P4VP-TC) as chain transfer agent. Methanol was selected because it is a solvent of P4VP but is a nonsolvent of PS. The P4VP-TC used in this study had a M_n = 10 400 g/mol and M_w/M_n = 1.08. When RAFT polymerization of St with a feed molar ratio of P4VP-TC/St (0.1 g)/2,2′-azobis(isobutyronitrile) (AIBN) = 10:5000:1 was carried out in methanol (1 g), the reaction solution displayed a transition from transparence to blue opalescence (Figure 1A), where the aggregates formed were spherical micelles with average diameter (D) of ∼80 nm measured by TEM (Figure 1D), and the morphology did not change after 24 h of polymerization due to very slow propagation of PS chains (Figure S1). Thus, high feed ratio of St to 4VP was used because St can act as monomer and also as a good solvent of PS before its polymerization. The St increased to 2 g with a feed ratio of P4VP-TC/St/AIBN = 10:100000:1 in methanol (1.1 g) at 80 °C; the clean polymerization system turned to blue opalescence, further to milk white (Figure 1B), where the morphology was vesicles with D of ∼280 nm obtained by TEM (Figure 1E). When the St continued to increase to 2.4 g, and the polymerization with a feed ratio of P4VP-TC/St/AIBN = 10:120000:1 was carried out in methanol (1 g) at 80 °C, the same apparent changes with that in Figure 1B was observed (Figure 1C), where the vesicles and the fused vesicles coexisted (Figure 1F).

Since the ratio of gyration (R_g) to hydrodynamic radius (R_h) is very sensitive to the morphology of aggregates,[8] the laser light scattering (LLS) was used to trace morphology transition in the polymerization. Generally, the R_g/R_h values for spheres, vesicles with thin wall, and vesicles with wall thickness of about 1/3 their outer radius are 0.77, 1.0, and 0.86, respectively.[9] So the RAFT polymerization with a feed molar ratio of P4VP/St(2 g)/AIBN = 10:100000:1 in methanol (1 g) was studied. As shown in Figure 2A, LLS curve of the reaction solution at 1 h displayed only one peak at R_h = 2.3 nm, which is ascribed to molecules of the P4VP-*b*-PS. As the polymerization proceeded for 2 h, the peak at 2.3 nm decreased greatly and a new peak at 15.7 nm appeared, and its R_g/R_h of ∼0.77 (Figure 2B) indicates the formation of the spherical micelles. For 4 h of polymerization, we can see two peaks: a big peak at R_h = 55.8 nm and a small one at 143 nm. The former is spherical micelles, and the latter may be vesicles because their peaks locate the positions similar to that for 3 and 12 h of polymerization, respectively (R_g/R_h cannot be used to identify the morphology because of bimodal distribution of the particles). After 12 h of polymerization, the peak of the spherical micelles disappeared completely, and only one peak appeared at R_h = 220 nm on the LLS curve. The vesicles did not change until 24 h of polymerization because the R_g/R_h values are 1.04 at 12 h and 1.09 at 24 h.

In order to further verify the phase separation and transition of morphology, transmission electron microscopy (TEM) was used to follow the same polymerization. The images of the aggregates formed at 2, 3, 4, 6, 12, and 24 h of polymerization are respectively shown in Figure 3A−F. The spherical micelles with D of 31 nm were formed at 2 h and then grew to D of 62 nm at 3 h. After 4 h of polymerization, a few particles began to adhere to one another, forming more stable and big size vesicles (D = ∼195 nm), but most aggregates kept spheres, and then more vesicles were formed (Figure 3D). All these are same with LLS result in Figure 2A. The transformation of the spheres into the vesicles completed at 12 h, and the vesicles with D of ∼320 nm were formed, which is similar to the SEM result in Figure S3. When the polymerization was prolonged to 24 h, the vesicles remained; their size was not changed obviously.

*Corresponding author. E-mail: pcy@ustc.edu.cn.

 Published on Web 07/02/2009

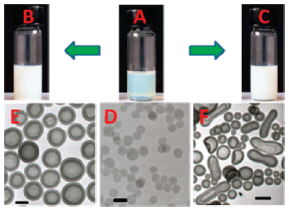

Figure 1. Optical photos of polymerization with different feed molar ratio of P4VP/St/AIBN: (A) 10:5000:1 (St: 0.1 g; CH_3OH: 1 g), (B) 10:100000:1 (St: 2 g; CH_3OH: 1.1 g), and (C) 10:120000:1 (St: 2.4 g; CH_3OH: 1 g). Temperature: 80 °C; time: 24 h. TEM images D, E, and F of the morphologies formed respectively from the polymerization A, B, and C. Scale bars: D, 100 nm; E, 200 nm; F, 500 nm.

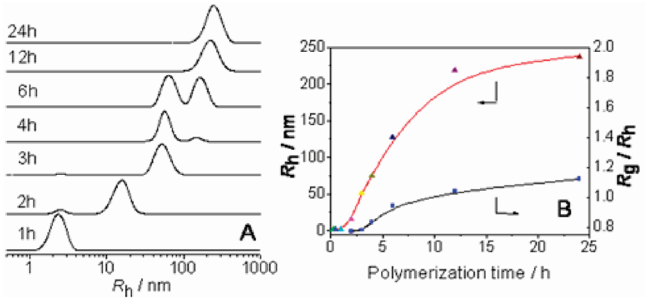

Figure 2. (A) LLS curves at different polymerization times (the scattering angle θ: 15°). (B) Relationship of R_h and R_g/R_h with the polymerization time. The correlation method of "unweighted" was used for calculation of particles size. Feed molar ratio of P4VP/St/AIBN = 10/100000/1; St: 2 g; CH_3OH: 1 g; 80 °C.

For understanding the morphology transition, nuclear magnetic resonance (NMR) and gel permeation chromatography (GPC) were used to trace the polymerization. The composition of the polymers formed was characterized by ^1H NMR spectra. As shown in Figure S2, the characteristic proton signals of pyridine in P4VP and phenyl ring in PS appeared at 8.31, 6.36 and 7.07, 6.57 ppm, respectively. With progress of the polymerization, the signal at 8.31 ppm decreased and the signal at 7.07 ppm increased, which indicates the length ratio increase of PS to P4VP chains. On the basis of the degree of polymerization (DP) of P4VP and integration ratio of the signal at 8.31 ppm to that at 7.07 ppm, the DPs of P4VP and PS segments were calculated. Before 2 h of reaction, the block copolymer was formed but dissolved in the reaction media. When the PS increased past a critical value of chain length forming the $P4VP_{99}$-*b*-PS_{394}, association of PS blocks was induced to form spherical micelles. This is the same with the reported results.[3−5] The main driving force is big change of chain length ratio of PS to P4VP (from 0 to 3.94), whereas the δ of the media changed very slightly (from $\delta = 22.9$ to 23). With progress of polymerization, PS blocks continued to grow (Figures S4 and S5). As DP of PS became 2040 for 4 h of polymerization, stretching of PS chains in the cores and the surface tension between the core and the outside solvent altered, and the spheres became unstable. They began to be coagulated and fused to form vesicles. Since their size distribution is broad (Figure 3A) due to different amounts of macromolecules in every micelle, the coagulation and fusion took place for ~8 h (Figure 2A). After rearrangement and continuous growth of the polymer chains in the wall of vesicles, the wall expanded and became thinner relative to the vesicles size. When DP of PS increased to 3800 at 12 h, the vesicles with approximately $D = 320$ nm and the wall thickness (~45 nm) were formed. Further polymerization did not alter the morphology; obvious size change was not observed (Figure 3E,F). At the same time, by tuning the feed ratio of RAFT polymerization, different vesicular morphologies could be prepared, as shown in Figure 4, which proved the generality of this method to prepare the vesicular nanomaterials.

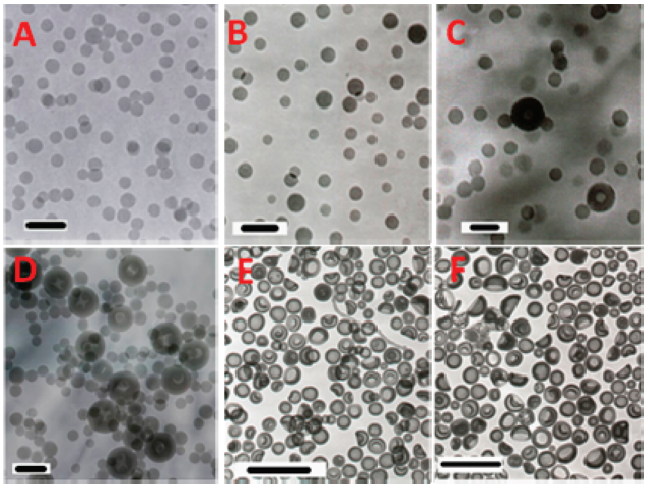

Figure 3. TEM images of the morphologies formed from different polymerization time: (A) 2, (B) 3, (C) 4, (D) 6, (E) 12, and (F) 24 h. P4VP/St/AIBN = 10:100000:1 (molar ratio); St: 2 g; CH_3OH: 1 g; 80 °C. Scale bars: (A) 100 nm, (B, C, D) 200 nm, (E, F) 1000 nm.

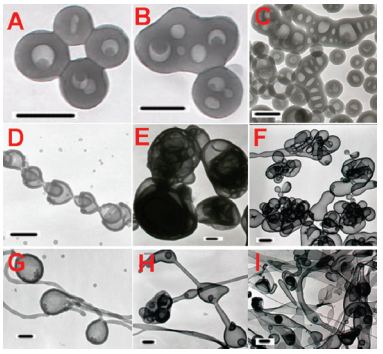

Figure 4. TEM images of multiple morphologies formed from RAFT polymerization with different feed molar ratios of P4VP-TC/St/AIBN: (A−D) 10/200000/1; P4VP-TC: 20 mg; CH_3OH: 0.5−2 g; (E−I) 10/100000−200000/1; P4VP: 20 mg; CH_3OH: 0.5−1.5 g; 80 °C; 24 h. Scale bar: 500 nm.

In summary, a facile and feasible approach for preparation of vesicular nanomaterials has been developed, and various morphologies are achieved by RAFT polymerization in a selective solvent with concentration as high as 0.5 g/mL. Formation of block copolymers, self-assembling, and morphology transition are accomplished in one-pot polymerization, and morphology transition is a key step for formation of the vesicular morphologies. This approach shows a great potential for preparation of nanostructural materials in large scale.

Acknowledgment. We thank the National Natural Science Foundation of China for financial support under Contracts 50673086 and 50633010. We also thank Ming Gong and Tan-Wei Li for the FETEM and TEM measurements.

Supporting Information Available: Text giving general experimental procedures. This material is available free of charge via the Internet at http://pubs.acs.org.

References and Notes

(1) (a) Axthelm, F.; Casse, O.; Koppenol, W. H.; Nauser, T.; Meier, W.; Palivan, C. G. *J. Phys. Chem. B* **2008**, *112*, 8211–8217. (b) Shum, H. C.; Kim, J.-W.; Weitz, D. A. *J. Am. Chem. Soc*. **2008**, *130*, 9543–9549. (c) Dean, J. M.; Verghese, N. E.; Pham, H. Q.; Bates, F. S. *Macromolecules* **2003**, *36*, 9267–9270. (d) Kim, Y.; Dalhaimer, P.; Christian, D. A.; Discher, D. E. *Nanotechnology* **2005**, *16*, S484–S491. (e) Yow, H. N.; Routh, A. F. *Soft Matter* **2006**, *2*, 940–949.

(2) (a) Du, J. Z.; Chen, Y. M.; Zhang, Y. H.; Han, C. C.; Fischer, K.; Schmidt, M. *J. Am. Chem. Soc*. **2003**, *125*, 14710–14711. (b) Yu, Y.; Eisenberg, A. *J. Am. Chem. Soc*. **1997**, *119*, 8383–8384. (c) Fu, J.; Luan, B.; Yu, X.; Cong, Y.; Li, J.; Pan, C. Y.; Han, Y. C.; Yang, Y.; Li, B. Y. *Macromolecules* **2004**, *37*, 976–986. (d) Zou, P.; Pan, C. Y. *Macromol. Rapid Commun*. **2008**, *29*, 763–771.

(3) Ji, W.; Yan, J.; Chen, E.; Li, Z.; Liang, D. *Macromolecules* **2008**, *41*, 4914–4919.

(4) Zheng, G. H.; Pan, C. Y. *Macromolecules* **2006**, *39*, 95–102.

(5) (a) Wan, W. M.; Pan, C. Y. *Macromolecules* **2007**, *40*, 8897–8905. (b) Zheng, Q.; Zheng, G. H.; Pan, C. Y. *Polym. Int*. **2006**, *55*, 1114–1123.

(6) Zhang, L.; Eisenberg, A. *J. Am. Chem. Soc*. **1996**, *118*, 3168–3181.

(7) Zhang, L.; Eisenberg, A. *Polym. Adv. Technol*. **1998**, *9*, 677–699.

(8) Burchard, W.; Richtering, W. *Prog. Colloid Polym. Sci*. **1989**, *80*, 151–163.

(9) (a) Dou, H. J.; Jiang, M.; Peng, H. S.; Chen, D. Y.; Hong, Y. *Angew. Chem., Int. Ed.* **2003**, *42*, 1516–1519. (b) Zhou, S. Q.; Wu, C. *Phys. Rev. Lett*. **1996**, *77*, 3053–3055.